

## Molecular and intramolecular dynamics of a C<sub>80</sub> dimetallofullerene

Wataru Sato, Keisuke Sueki, Koichi Kikuchi, Shinzo Suzuki, Yohji Achiba, and Hiromichi Nakahara  
*Graduate School of Science, Tokyo Metropolitan University, Hachioji, Tokyo 192-0397, Japan*

Yoshitaka Ohkubo

*Research Reactor Institute, Kyoto University, Kumatori, Osaka 590-0494, Japan*

Kichizo Asai

*Department of Applied Physics and Chemistry, The University of Electro-Communications, Chofu, Tokyo 182-8585, Japan*

Fumitoshi Ambe

*The Institute of Physical and Chemical Research (RIKEN), Wako, Saitama 351-0198, Japan*

(Received 5 June 1998)

Molecular and intramolecular dynamics of solid-state CeLa@C<sub>80</sub> has been studied based on time-differential perturbed-angular-correlation (TDPAC) measurements by employing the <sup>140</sup>Ce nucleus, a β<sup>-</sup> decay product of <sup>140</sup>La, as the probe. Rotational motion of the molecules was suggested by the temperature dependence of the reorientational correlation time of electric quadrupole interaction τ<sub>c</sub>, which abruptly changes at approximately 160 K, implying the freezing of the motion. The dynamic motion of the Ce atom was observed even below that temperature, down to 40 K, and all of the motions causing dynamic perturbation on the nucleus vanish at further low temperatures. Some intrinsic nature of the interactions among and within the fullerene molecules, CeLa@C<sub>80</sub>, is also discussed in comparison with Ce@C<sub>82</sub>, based on physical parameters obtained by the TDPAC method. [S0163-1829(98)09639-8]

### I. INTRODUCTION

Dynamic behavior of endohedral metallofullerenes has been investigated from various possible aspects, experimentally and theoretically, since macroscopic production of those species was successfully achieved,<sup>1</sup> and some noteworthy information pertaining to the nature of the dynamics, such as the reorientational correlation time and activation energy for thermally activated molecular rotations, has been obtained by means of various spectroscopic methods.<sup>2-5</sup> Among recent reports on metallofullerene dynamics, behavior of endohedral metal atoms has been of great interest as well as molecular motion. As regards Sc<sub>2</sub>@C<sub>84</sub> at room temperature, for example, intramolecular oscillatory dynamics of the endohedral metal atoms and quenching of the molecular rotation of the species in the form of powder have been suggested by the electron density distribution obtained by a maximum entropy method.<sup>4</sup> Intramolecular circulating motion of encapsulated atoms at room temperature has been suggested for La<sub>2</sub>@C<sub>80</sub> in *o*-dichlorobenzene solution based on a combined linewidth analysis of <sup>13</sup>C- and <sup>139</sup>La-NMR (where NMR is nuclear magnetic resonance).<sup>6</sup> Theoretical calculation supports those interpretations on the distinctive dynamics of these fullerenes ascribing the difference of the mode of the internal motion between the two molecules to the difference of the potential barriers where the metal atoms (Sc and La) are accommodated in energetically optimum condition.<sup>7</sup> With respect to solid-state dynamics of dimetallofullerenes such as molecular rotation, however, there have been few reports for reasons such as these: difficulty in preparing those species in macroscopic quantities, and lack of appropriate analytical methods for each individual species, and so forth.

It is, in particular, important to investigate the molecular

and intramolecular dynamics of solid-state dimetallofullerenes so as to obtain information concerning the interactions between molecules and between endohedral atoms and the ambient cage. In order to elucidate the dynamic nature of dimetallofullerenes, we adopted a time-differential perturbed angular correlation (TDPAC) method for the species following our previous work.<sup>5</sup> It was found in the work that the TDPAC method is exceedingly well suited for the investigation of the dynamic nature of endohedrally doped fullerenes because it allows simultaneous determination of significant physical quantities such as the electric-field gradient (EFG) produced at the probe nucleus and the reorientational correlation time of the principal axis of the EFG. For the purpose of probing into the molecular and intramolecular dynamics of dimetallofullerenes in detail, we performed TDPAC measurements for CeLa@C<sub>80</sub>, a β<sup>-</sup> decay product of <sup>140</sup>La<sup>139</sup>La@C<sub>80</sub>, which is produced in a reactor by the neutron capture reaction of <sup>139</sup>La<sub>2</sub>@C<sub>80</sub>, and succeeded in observing the detailed dynamic nature of the engaged metal atoms and the molecule as a whole. In the present paper, not only the dynamics but also estimated physical quantities, such as the nuclear quadrupole frequency, are also discussed in comparison with those for Ce@C<sub>82</sub> obtained in the previous work.

### II. EXPERIMENT

#### A. Sample preparation

##### 1. Production of La<sub>2</sub>@C<sub>80</sub>

For macroscopic production of carbon soot containing La fullerenes, an arc discharge of the cathode electrode, a sin-

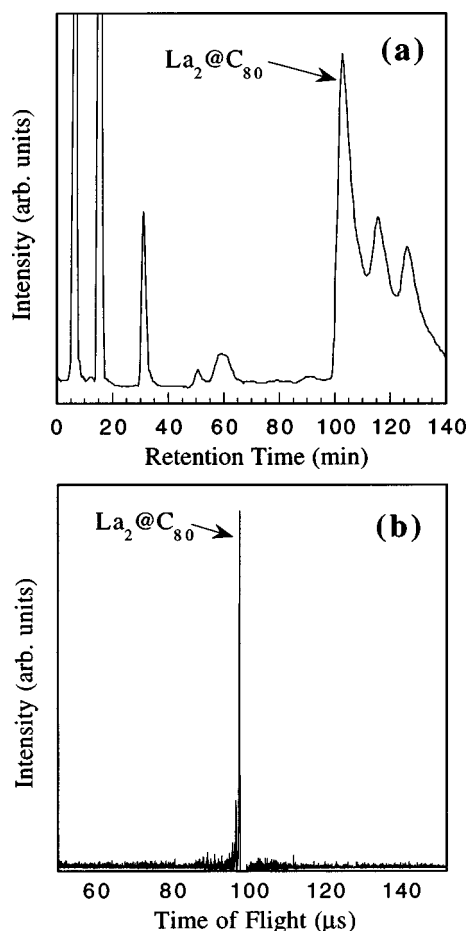


FIG. 1. (a) HPLC elution curve of the  $\text{La}_2@C_{80}$ -containing fraction collected at the first-stage separation. (b) Laser-desorption time-of-flight mass spectrum for the peak fraction containing  $\text{La}_2@C_{80}$  obtained by the second-stage HPLC purification (a).

tered carbon rod initially consisting of a 1% w/w mixture of lanthanum oxide ( $\text{La}_2\text{O}_3$ ) in graphite, was carried out under a 250-Torr He atmosphere at a discharge current setting of 250 A in the dc mode. After recovering the produced soot, it was dissolved in *o*-dichlorobenzene and refluxed for approximately 10 h under a nitrogen atmosphere. Fullerene ingredients soluble in the solvent were extracted from the soot: approximately 1% yield over the total soot.

In order to extract and purify the species of interest,  $\text{La}_2@C_{80}$ , a two-stage high-performance liquid chromatography (HPLC) separation was performed with two different columns. At the first stage, a buckyprep column (20 mm  $\phi \times 250$  mm; Cosmosil, Nacalai Tesque Inc.) was used for a rough separation of the fraction containing  $\text{La}_2@C_{80}$  at the retention time of 68–78 min, and then, at the second stage, a 5PBB column (20 mm  $\phi \times 250$  mm; Cosmosil, Nacalai Tesque Inc.) for a further purification of  $\text{La}_2@C_{80}$  in the fraction collected at the first stage. For both of the separation, toluene was used as the eluent with the flow rate of 12 ml/min. The elutions were monitored by UV absorption spectrometers at a wavelength of 340 nm. The elution curve for the second-stage purification is shown in Fig. 1(a) indicating the peak fraction of  $\text{La}_2@C_{80}$  eluted at around 103 min. The species recovered at the retention time of 99–108 min was ascertained to be pure  $\text{La}_2@C_{80}$  by laser-

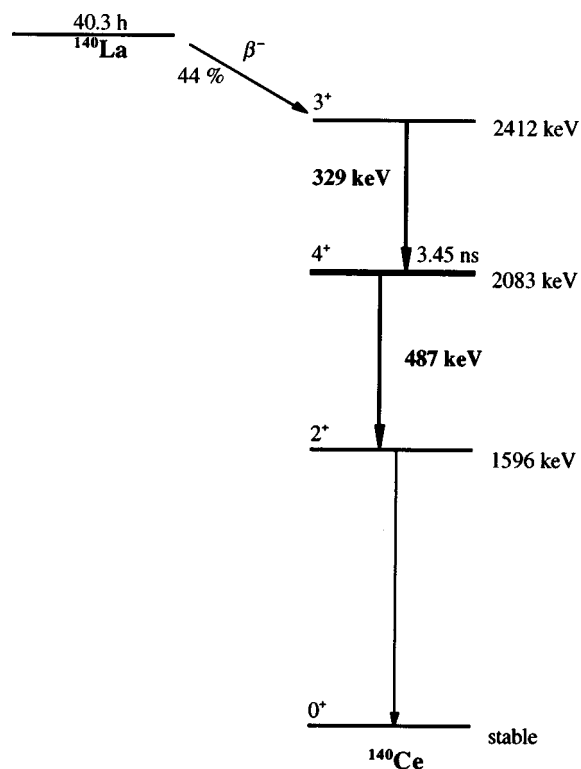


FIG. 2. Simplified decay scheme of  $^{140}\text{Ce}(\leftarrow^{140}\text{La})$  for the relevant cascade.

desorption time-of-flight mass spectrometry as shown in Fig. 1(b).

## 2. Source preparation

After removing the solvent by evaporation, about 1 mg of the purified powder sample was sealed in a quartz tube of 2 mm  $\phi$  under reduced pressure. The sample in the tube was irradiated with reactor neutrons with the neutron fluence rate of  $1 \times 10^{14} \text{ cm}^{-2} \text{ s}^{-1}$  for 24 h, and radioactive  $^{140}\text{La}^{139}\text{La}@C_{80}$  was produced by the  $^{139}\text{La}(n, \gamma)^{140}\text{La}$  reaction. After the irradiation, the sample was dissolved in carbon disulfide and filtrated with a membrane filter so as to get rid of the impurities produced by hot atom effects and/or radiation effects. Then the sample underwent a further HPLC purification with a 5PBB column, giving a yield of approximately 10% over the irradiated amount, and the powder sample for TDPAC measurements was finally prepared. (The above-mentioned impurities, species adsorbed in the inner surface of the quartz tube, and others constitute the other 90%.)

## B. TDPAC measurements

TDPAC measurements were performed on the  $\gamma$ - $\gamma$  cascade of 329–487 keV from excited  $^{140}\text{Ce}$  nucleus<sup>8</sup> (Fig. 2) at various temperatures (423, 373, 323, 290, 240, 200, 160, 120, 100, 80, 70, 40, 20, and 10 K) in order to examine the temperature dependence of the time-differential anisotropy. For the high- and low-temperature measurements, the source was set in an electric furnace and a cryostat equipped with temperature controllers, respectively. The directional anisotropy of the angular correlations of the  $\gamma$  rays was observed at

$\pi/2$  and  $\pi$  directions with a conventional four-detector system. For the fast-slow coincidence detection, BaF<sub>2</sub> scintillation counters of 1.5 in  $\phi \times 1$  in were arranged at a distance of 3 cm from the source. The time resolution of the system was estimated to be 300–400 ps based on the full width at half-maximum of a peak for prompt coincidence. After subtracting accidental coincidence counts from each time spectrum and correcting the solid angle of the scintillators, directional anisotropies at each temperature were derived. (We verified the propriety of the estimate of the background by checking the raw data of each time spectrum.)

### III. DESCRIPTION OF TDPAC FOR <sup>140</sup>Ce( $\leftarrow$ <sup>140</sup>La)

For the case in which the angular correlation of the successive  $\gamma$  rays is perturbed by randomly oriented extranuclear field while the probe nucleus stays at the intermediate state of the cascade (2083 keV and 4<sup>+</sup> for the present transition), the directional correlation function,  $W(\theta, t)$ , of the  $\gamma$  rays is described by the following equation:

$$W(\theta, t) = 1 + A_{22}G_{22}(t)P_2(\cos \theta), \quad (1)$$

where  $\theta$  is the angle between the directions of the cascade  $\gamma$  rays,  $A_{22}$  ( $= -0.14$  for the present cascade) is the correlation coefficient of the second term of the Legendre polynomials,  $P_2(\cos \theta)$ ,  $G_{22}(t)$  is the time-differential perturbation factor, and  $t$  is the time interval between the cascade. Here higher terms than the second order were neglected because  $A_{22} \gg A_{44}$ . When a four-detector system is employed for the coincidence detection, the directional anisotropy,  $A_{22}G_{22}(t)$ , is given by a simple arithmetic operation as follows:

$$A_{22}G_{22}(t) = \frac{2[N(\pi, t) - N(\pi/2, t)]}{N(\pi, t) + 2N(\pi/2, t)}, \quad (2)$$

where  $N(\theta, t) [\propto W(\theta, t)\exp(-t/\tau_N)]$ , where  $\tau_N$  is the mean life of the intermediate state] is the number of coincident events observed at angle,  $\theta$ .

The coefficient  $A_{22}$  is characteristic of the multipolarities of the cascade  $\gamma$  rays and the nuclear spins of sublevels relevant to the cascade transitions.<sup>9</sup> The information pertaining to the extranuclear field is provided by the factor  $G_{22}(t)$ . For the case in which the probe nucleus has a static electric quadrupole interaction with an axially symmetric EFG produced by the extranuclear charge distribution,  $G_{22}(t)$  is explicitly expressed as

$$\begin{aligned} G_{22}^{\text{static}}(t) = & \frac{1}{3465}[993 + 30 \cos(3\omega_Q t) + 243 \cos(9\omega_Q t) \\ & + 540 \cos(12\omega_Q t) + 525 \cos(15\omega_Q t) \\ & + 588 \cos(21\omega_Q t) + 378 \cos(24\omega_Q t) \\ & + 168 \cos(36\omega_Q t)] \end{aligned} \quad (3)$$

for the relevant transition, where  $\omega_Q$  represents the nuclear quadrupole frequency of the intermediate state under EFG.

When the correlation time  $\tau_c$  for the reorientation of the principal axis of the EFG is sufficiently shorter than  $1/\omega_Q$ ,

according to the diffusion approximation deduced by Abragam and Pound,<sup>10</sup> the directional anisotropy shows exponential-type attenuation following the equation

$$G_{22}(t) = \exp(-\lambda t). \quad (4)$$

Here,  $\lambda$  is the relaxation constant, which is written in the next form in case of the electric quadrupole interaction:<sup>10</sup>

$$\lambda = \frac{3}{5}\tau_c\omega_Q^2 k(k+1)[4I(I+1) - k(k+1) - 1], \quad (5)$$

where  $k$  ( $=2$  for the present case) stands for the term number as in the Legendre polynomials,  $P_k(\cos \theta)$ , and  $I$  ( $=4$  for the 2083-keV state of <sup>140</sup>Ce) is the nuclear total angular-momentum quantum number of the intermediate state of the cascade.

### IV. RESULTS AND DATA ANALYSIS

TDPAC for the polycrystalline powder CeLa@C<sub>80</sub> observed at various temperatures are shown in Fig. 3.

At high temperatures from 200 to 423 K, the directional anisotropies  $A_{22}G_{22}(t)$  show exponential-type attenuation seemingly following Eq. (4). Taking a survey of each high-temperature TDPAC, however, the directional anisotropies do not seem to approach zero asymptotically even after a long elapsing time in the intermediate state. This incomplete attenuation is considered to be attributed to the presence of the second component in each TDPAC in a similar way to the case of Ce@C<sub>82</sub>.<sup>5</sup> On the analogy of the analysis of Ce@C<sub>82</sub> in the high-temperature range, accordingly, least-squares fits were performed with the following equation:

$$A_{22}G_{22}(t) = -0.14[P \exp(-\lambda_1 t) + (1-P)\exp(-\lambda_2 t)], \quad (6)$$

where  $P$  is the fraction of the first major component, and the subscripts 1 and 2 represent the first and second components, respectively.

As for the medium-temperature range 40–160 K, each TDPAC has a damped oscillatory structure, which implies the nuclear precession caused by a quasistatic perturbation from the extranuclear field. The coexistence of two different components is also assumed for this temperature range because the minor component constructing a backgroundlike low plateau observed in the high-temperature range is still present in the TDPAC. Taking the minor component to be contributing to the medium-temperature TDPAC in the same way as the high-temperature ones, least-squares fits were carried out by

$$\begin{aligned} A_{22}G_{22}(t) = & -0.14[P \exp(-t/\tau_c)G_{22}^{\text{static}}(t) \\ & + (1-P)\exp(-\lambda_2 t)], \end{aligned} \quad (7)$$

where the relaxation for the first component is taken into account with the adiabatic approximation<sup>11</sup> in the form of  $\exp(-t/\tau_c)$  so as to reproduce the damped oscillation.

At 10 and 20 K, the lines drawn by Eq. (7) do not reproduce the observed  $A_{22}G_{22}(t)$  well. Both spectra were reasonably fitted on the assumption of the static perturbation factor with Gaussian distribution<sup>12</sup> of  $\omega_Q$ , instead. The validity of

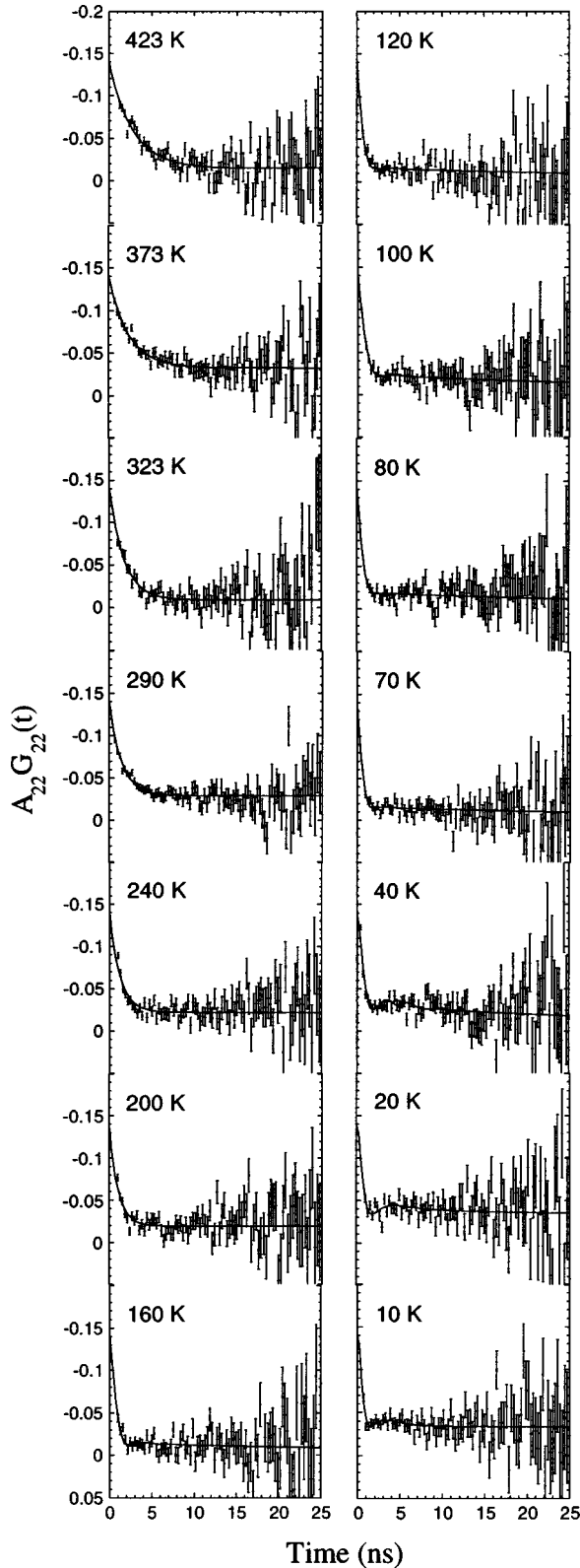


FIG. 3. TDPAC of  $^{140}\text{Ce}(\leftarrow^{140}\text{La})$  in  $\text{CeLa@C}_{80}$  at various temperatures. Each time-variant anisotropy at high temperatures (200–423 K), medium temperatures (40–160 K), and low temperatures (10 and 20 K) is fitted with least squares by using Eqs. (6), (7), and (8), respectively.

the fits can be confirmed by the residual anisotropy after a long elapsing time in the intermediate state of the cascade, which is close to the so-called core value [ $\cong -0.14$

TABLE I. Parameters obtained by least-squares fits with Eqs. (6), (7), and (8) in the text. The average values for the quadrupole frequency  $\langle\omega_Q\rangle$  were calculated based on the  $G_{22}^{\text{static}}(t)$  at each low-temperature TDPAC for both species.

	$\langle\omega_Q\rangle$ ( $10^7$ rad $\text{s}^{-1}$ )	$\langle P\rangle$	$E_a$ ( $\text{kJ mol}^{-1}$ )
$\text{Ce@C}_{82}$	$6.5 \pm 0.3$	$0.40 \pm 0.03$	$1.3 \pm 0.1$
$\text{CeLa@C}_{80}$	$11 \pm 2$	$0.84 \pm 0.07$	$3.2 \pm 0.2$

( $=A_{22}$ ) $\times 993/3465$  for the present case]. Since the low plateaus are still observed at these low temperatures, the TDPAC were fitted by the following equation by assuming the presence of the second component as well:

$$A_{22}G_{22}(t) = -0.14[P G_{22}^{\text{static}}(t)_{\delta\omega_Q} + (1-P)\exp(-\lambda_2 t)], \quad (8)$$

where

$$G_{22}^{\text{static}}(t)_{\delta\omega_Q} = a_0 + \sum_{i=1}^7 a_i \exp(-\frac{1}{2}\delta^2\omega_{Qi}^2 t^2) \cos \omega_{Qi} t, \quad (9)$$

when Eq. (3) is expressed in a general form as

$$G_{22}^{\text{static}}(t) = a_0 + \sum_{i=1}^7 a_i \cos \omega_{Qi} t. \quad (10)$$

The relative width  $\delta$  is defined by  $\delta = \sigma/\omega_{Qi}^0$ , where  $\sigma$  is the width of the distribution and  $\omega_{Qi}^0$  is the centroid of  $\omega_Q$  for each term. For both of the low-temperature spectra,  $\delta \cong 50\%$ .

The mean fraction of the minor second component denoted by  $[1 - \langle P \rangle]$  was so small that reliable values for the relaxation constant  $\lambda_2$  could not be obtained. The parameters for all the temperature range were, therefore, fixed at certain reasonable values so that their minor variations do not affect the analytical results for the first component. The fitted lines by Eqs. (6), (7), and (8) are shown in each of the TDPAC. The mean values of respective parameters,  $\langle\omega_Q\rangle$  and  $\langle P \rangle$ , optimized by the fits are tabulated in Table I. The activation energies in the table are discussed in the next section.

## V. DISCUSSION

Concerning the stability of dimetallofullerenes, both  $\text{La}_2\text{@C}_{80}$  and  $\text{Ce}_2\text{@C}_{80}$  have already been reported to be air stable,<sup>13,14</sup> and, from the similarity of their UV-Vis absorption spectra,<sup>14,15</sup> it can be considered that both pairs of the encapsulated atoms are stabilized in the identical  $\text{C}_{80}$  cage. It would be, therefore, reasonable to regard  $\text{CeLa@C}_{80}$  produced by the  $\beta^-$  particle emission from  $\text{La}_2\text{@C}_{80}$  as a stable species as well.<sup>16</sup>

As stated at the end of the preceding section, it is difficult to discuss the temperature dependence of  $\lambda_2$ , especially in the present case because of the small mean fraction of the minor component,  $[1 - \langle P \rangle]$ ; this is different from the case for  $\text{Ce@C}_{82}$  because the second component whose anisotropy slowly attenuates occupies approximately as much as 60%, which allows discussing the temperature dependence.<sup>5</sup> In the following, accordingly, only the first component, which occupies the major fraction, is discussed in detail.

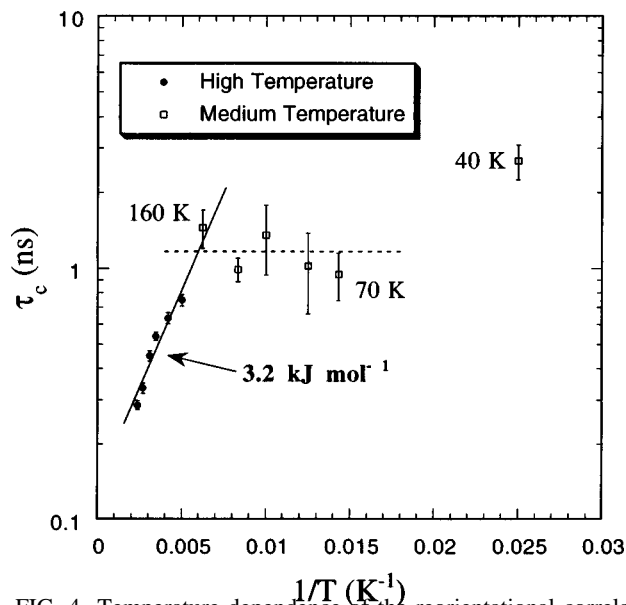


FIG. 4. Temperature dependence of the reorientational correlation time  $\tau_c$  at high and medium temperatures. The dashed horizontal line indicates the average value of each  $\tau_c$  estimated at medium temperatures, except for 40 K.

## A. Molecular and intramolecular dynamics

### 1. Molecular motion

The reorientational correlation time,  $\tau_c$ , estimated by the least-squares fits for 40 to 423 K is plotted as a function of reciprocal temperature  $1/T$  in Fig. 4. The values for the high-temperature range were obtained by a calculation with Eq. (5) by substituting the mean nuclear quadrupole frequency  $\langle\omega_Q\rangle$  given in Table I for  $\omega_Q$ . As in the case for Ce@C<sub>82</sub>, the  $\tau_c$  values become larger with decreasing temperature in the high-temperature range. This temperature-dependent phenomenon is, therefore, reasonably interpreted as slow-down of the thermally activated motion of the extranuclear field against the probe nucleus. By analogy with the molecular rotations of Ce@C<sub>82</sub> and of some other fullerenes,<sup>17–21</sup> we consider that the perturbation is mostly attributed to the dynamic motion of CeLa@C<sub>80</sub> molecules because of a similar temperature dependence to that of Ce@C<sub>82</sub>, and its abrupt change at approximately 160 K directly implies the freeze of the motion. This presumption is supported by the observation that those TDPAC obtained at medium temperatures have similar time variation to that for CeLa@C<sub>80</sub> in 1,2,4-trichlorobenzene solution at 240 K, which is below the freezing point (290 K) of the solvent (Fig. 5).

### 2. Intramolecular motion

In Fig. 4, contrary to the high-temperature range, little, if any, temperature dependence is seen in the  $\tau_c$  values for the range below the freezing temperature, although the TDPAC for this temperature range still obviously indicates relaxation signifying a further dynamic perturbation. It is plausibly inferred, as presumed for the case of Ce@C<sub>82</sub>, that the motion causing this perturbation is initiated by the recoil effect triggered by the  $\beta^-$  particle emission from the <sup>140</sup>La nucleus because, considering the small temperature dependence, it would be difficult to interpret the dynamic motion as ther-

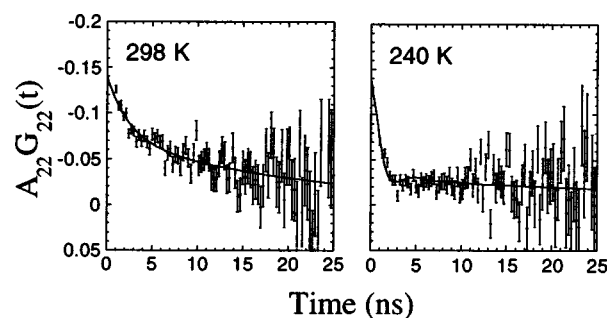


FIG. 5. TDPAC of <sup>140</sup>Ce ( $\leftarrow$  <sup>140</sup>La) in CeLa@C<sub>80</sub> 1,2,4-trichlorobenzene solution at 298 and 240 K. Each time-variant anisotropy is fitted with Eqs. (6) and (7), respectively.

mally activated. The relaxation represented by the damping factor,  $\exp(-t/\tau_c)$ , in Eq. (7), is possibly due to intramolecular circular motion of the Ce atom. Since the potential barrier is, according to a theoretical calculation,<sup>7</sup> considerably low (approximately 5 kcal/mol) owing to the spherical structure with an  $I_h$  symmetry of the ambient carbon cage, it can be considered that the low barrier enables the endohedral Ce atom to have the circular motion with small temperature dependence together with the neighbor La even at quite low temperatures.

From the observation of the longer correlation time of approximately 3 ns as indicated in Fig. 4, 40 K appears to be a transition temperature to the freezing of the intramolecular dynamic motion in the time scale of the present TDPAC measurements. Assuming the recoil effect to be the trigger of the intramolecular motion at the medium temperatures, the fast recoil-energy dissipation is a conceivable cause of this freezing phenomenon.<sup>22</sup> The kinetic energy for the motion of the Ce atom would be limited as a result of the fast energy dissipation to the lattice surrounding the atom; consequently, the intramolecular motion slows down.

At further low temperatures, 20 and 10 K, it is shown in the TDPAC that all the dynamic motions vanish and the directional anisotropy,  $A_{22}G_{22}(t)$ , for the first component is reproduced only by a static perturbation factor with Gaussian distribution of  $\omega_Q$ . This observation could indicate that the Ce atom stays in the minimum potential for the time scale of these TDPAC measurements at these low temperatures, having a static interaction between the nuclear quadrupole moment and the extranuclear field. The damped oscillation reproduced by the Gaussian distribution is presumably ascribed to some vibrational motion within the minimum potential. This phenomenon is in contrast to the case of Ce@C<sub>82</sub>, where slow attenuation of the directional anisotropy can be seen even at 10 K, implying intramolecular loop motion of the endohedral Ce atom. Regarding CeLa@C<sub>80</sub>, the quenching of the intramolecular atomic motion could be due to the presence of the counterpart La atom; the atom would be a considerable hindrance to the motion.

## B. Comparison of $E_a$ , $\tau_c$ , and $\omega_Q$ between Ce@C<sub>82</sub> and CeLa@C<sub>80</sub>

### 1. Activation energy

The activation energy for the molecular motion at the high temperatures was estimated to be  $3.2 \pm 0.2$  kJ mol<sup>-1</sup> by a least-squares fit of the  $\tau_c$  values on an Arrhenius-type equation:

TABLE II. Temperature variation of the reorientational correlation time for Ce@C<sub>82</sub> and CeLa@C<sub>80</sub>.

	$\tau_c$ (ns)			
	Room temp.	240 K	200 K	160 K
Ce@C <sub>82</sub>	0.32±0.03	0.38±0.04	0.58±0.06	0.89±0.09
CeLa@C <sub>80</sub>	0.54±0.02	0.63±0.03	0.75±0.04	1.5 ±0.3

$$\tau_c = A \exp(E_a/RT), \quad (11)$$

where  $A$  is a constant,  $E_a$  is the activation energy, and  $R$  is the gas constant. The estimated value is approximately 2.5 times as large as that for Ce@C<sub>82</sub>,<sup>5</sup> which implies that CeLa@C<sub>80</sub> needs more energy for its thermal motion than Ce@C<sub>82</sub>. It is therefore considered that each molecule of solid CeLa@C<sub>80</sub> has stronger interaction with outer surrounding molecules than that of Ce@C<sub>82</sub>.

### 2. Reorientational correlation time

In connection with molecular interaction, the reorientational correlation time  $\tau_c$ , could also be an index for discussing the thermal motion of the molecule. Table II indicates  $\tau_c$  values optimized in the least-squares fits of the time-differential  $A_{22}G_{22}(t)$  for the temperature range at which presumed molecular motion is observed for both of the species (160 K to room temperature). The values for Ce@C<sub>82</sub> were calculated in the same way as those for CeLa@C<sub>80</sub> by substituting the  $\langle\omega_Q\rangle$  value [ $= (6.5 \pm 0.3) \times 10^7 \text{ rad s}^{-1}$ ]<sup>5</sup> for  $\omega_Q$  in Eq. (5). It is obvious from the table that the  $\tau_c$  for CeLa@C<sub>80</sub> are, on average, about 64% larger than those for Ce@C<sub>82</sub>. These data evidently show the slower motion of the CeLa@C<sub>80</sub> molecule than that of the Ce@C<sub>82</sub>, which is consistent with the results regarding the activation energy in terms of the mobility of the molecules.

### 3. Nuclear quadrupole frequency

The difference of the nuclear quadrupole frequency  $\omega_Q$  can also be seen between CeLa@C<sub>80</sub> and Ce@C<sub>82</sub> as listed in Table I. As is obvious in the table,  $\langle\omega_Q\rangle$  for CeLa@C<sub>80</sub> is 1.7 times as large as that for Ce@C<sub>82</sub>, reflecting the difference of the magnitude of the EFG produced at the probe nucleus. As far as Ce@C<sub>82</sub> is concerned, the EFG at the probe nucleus is produced by the contribution of the polarization effect of the valence electrons and outer surrounding charge distribution, which are supposedly delocalized electrons over the  $\pi$  orbitals of the ambient carbon cage. The Ce nucleus as in the cage of CeLa@C<sub>80</sub>, however, is in electrically different circumstances, having a neighbor atom La, which is considered to be ionic and charged positively. It is considered as a qualitative interpretation that this positively charged atom should make a marked contribution toward producing additional EFG at the nucleus, and in consequence, the EFG observed for CeLa@C<sub>80</sub> is greater than that for Ce@C<sub>82</sub>. Another contribution toward the EFG could also be made on the assumption that the Ce atom is located closer to the wall of the carbon cage, compared with the case for Ce@C<sub>82</sub>, by the electrostatic repulsion between the en-

caged Ce and La atoms, and the nucleus feels a larger EFG by the lattice electrons because of their shorter distance from the nucleus.

## VI. SUMMARY AND CONCLUSION

The TDPAC measurements for an endohedral dimetallofullerene, CeLa@C<sub>80</sub>, have provided some valuable information pertaining to the intrinsic properties, such as the nature of molecular and intramolecular dynamic motions as well as the magnitude of the electric-field gradient, which are considerably difficult to be revealed by other analytical and/or spectroscopic methods.

As regards the whole molecular dynamics, we have found that the molecules even in the state of solid have a thermally activated motion with a temperature dependence at high temperatures. The dynamic motion slows down with decreasing temperature, and finally freezes at approximately 160 K, which is higher than the freezing point of the molecular rotation of Ce@C<sub>82</sub> (=approximately 80 K).

A dynamic motion has also been observed at medium temperature range from 40 to 160 K. From the observation that this movement has little, if any, temperature dependence, it can be considered that the recoil effect triggered by the  $\beta^-$  particle emission from the excited La nucleus initiates an intramolecular loop motion. The observation also suggests that the loop motion can last for at least the time scale of the present TDPAC measurements by possibly overcoming the potential ripples on the inner wall of the carbon cage as suggested by theoretical calculations. The TDPAC at 40 K, however, obviously indicates a phenomenon that the motion slows down transitionally to the motional freezing showing a long reorientational correlation time  $\tau_c$  ( $\approx 3$  ns).

At lower temperatures, 10 and 20 K, both of the TDPAC's show that all of the presumed motions vanish and a static interaction between the Ce nucleus and the extranuclear field has been observed.

Comparison studies on the activation energy  $E_a$  and the reorientational correlation time  $\tau_c$  have elucidated the nature of interaction between the molecules: the molecular motion of CeLa@C<sub>80</sub> is slower and needs more energy for the rotation than that of Ce@C<sub>82</sub>, which is also supported by the difference of the freezing temperatures of the molecular motions.

The electric field gradient at the Ce nucleus in CeLa@C<sub>80</sub> has been found to be larger than that in Ce@C<sub>82</sub>. This fact can be explained by the presence of the positively charged neighbor La atom contributing to the EFG, resulting in the greater EFG than that for Ce@C<sub>82</sub>.

In the present work, only the first component, which occupies the major fraction, has been discussed in detail. In order to elucidate the nature of the minority, further investigation with better counting statistics will be needed.

## ACKNOWLEDGMENTS

The authors are grateful for helpful advice from Professor M. Katada and for an important suggestion from Professor S. Nagase. They also thank Professor Y. Kawase and Dr. S. Uehara for their arrangement for the experiment. W.S. would like to express his gratitude to Dr. T. Kodama for his instruc-

tion and cooperation in the sample preparation. The present work was accomplished as part of the Inter-University Program for the Common Use of JAERI (Japan Atomic Energy Research Institute) Facilities and the Visiting Researcher's

Program of the Kyoto University Research Reactor Institute (KURRI). This work was partly supported by a grant from the Ministry of Education, Culture, Sports, and Science of Japan.

- 
- <sup>1</sup>W. Krätschmer, L. D. Lamb, K. Fostiropoulos, and D. R. Huffman, *Nature (London)* **347**, 354 (1990).
- <sup>2</sup>M. Rübsam, M. Plüschau, P. Schweitzer, K.-P. Dinse, D. Fuchs, H. Rietschel, R. H. Michel, M. Benz, and M. M. Kappes, *Chem. Phys. Lett.* **240**, 615 (1995).
- <sup>3</sup>Y. Miyake, S. Suzuki, Y. Kojima, K. Kikuchi, K. Kobayashi, S. Nagase, M. Kainosho, Y. Achiba, Y. Maniwa, and K. Fisher, *J. Phys. Chem.* **100**, 9579 (1996).
- <sup>4</sup>M. Takata, E. Nishibori, B. Umeda, M. Sakata, E. Yamamoto, and H. Shinohara, *Phys. Rev. Lett.* **78**, 3330 (1997).
- <sup>5</sup>W. Sato, K. Sueki, K. Kikuchi, K. Kobayashi, S. Suzuki, Y. Achiba, H. Nakahara, Y. Ohkubo, F. Ambe, and K. Asai, *Phys. Rev. Lett.* **80**, 133 (1998).
- <sup>6</sup>T. Akasaka, S. Nagase, K. Kobayashi, M. Wälchli, K. Yamamoto, H. Funasaka, M. Kato, T. Hoshino, and T. Erata, *Angew. Chem. Int. Ed. Engl.* **36**, 1643 (1997).
- <sup>7</sup>K. Kobayashi, S. Nagase, and T. Akasaka, *Chem. Phys. Lett.* **261**, 502 (1996).
- <sup>8</sup>*Table of Isotopes*, 8th ed., edited by R. B. Firestone and V. S. Shirley (Wiley, New York, 1996), Vol. 1.
- <sup>9</sup>H. Frauenfelder and R. M. Steffen, in  *$\alpha$ -,  $\beta$ -, and  $\gamma$ -Ray Spectroscopy*, edited by K. Siegbahn (North-Holland, Amsterdam, 1974), Vol. 2, p. 1198.
- <sup>10</sup>A. Abragam and R. V. Pound, *Phys. Rev.* **92**, 943 (1953).
- <sup>11</sup>A. G. Marshall and C. F. Meares, *J. Chem. Phys.* **56**, 1226 (1972).
- <sup>12</sup>H. Frauenfelder and R. M. Steffen, in  *$\alpha$ -,  $\beta$ -, and  $\gamma$ -Ray Spectroscopy* (Ref. 9), p. 1121.
- <sup>13</sup>T. Suzuki, Y. Maruyama, T. Kato, K. Kikuchi, Y. Nakao, Y. Achiba, K. Kobayashi, and S. Nagase, *Angew. Chem. Int. Ed. Engl.* **34**, 1094 (1995).
- <sup>14</sup>J. Ding and S. Yang, *Angew. Chem. Int. Ed. Engl.* **35**, 2234 (1996).
- <sup>15</sup>K. Kikuchi, Y. Nakao, Y. Achiba, and M. Nomura, *Fullerenes*, edited by K. M. Kadish and R. S. Ruoff (The Electrochemical Society, Pennington, NJ, 1994), 1077.
- <sup>16</sup>K. Kikuchi, K. Kobayashi, K. Sueki, S. Suzuki, H. Nakahara, Y. Achiba, K. Tomura, and M. Katada, *J. Am. Chem. Soc.* **116**, 9775 (1994).
- <sup>17</sup>C. S. Yannoni, R. D. Johnson, G. Meijer, D. S. Bethune, and J. R. Salem, *J. Phys. Chem.* **95**, 9 (1991).
- <sup>18</sup>R. Tycko, R. C. Haddon, G. Dabbagh, S. H. Glarum, D. C. Douglass, and A. M. Mujsce, *J. Phys. Chem.* **95**, 518 (1991).
- <sup>19</sup>R. Tycko, G. Dabbagh, R. M. Fleming, R. C. Haddon, A. V. Makhija, and S. M. Zahurak, *Phys. Rev. Lett.* **67**, 1886 (1991).
- <sup>20</sup>Y. Maniwa, K. Mizoguchi, K. Kume, K. Kikuchi, I. Ikemoto, S. Suzuki, and Y. Achiba, *Solid State Commun.* **80**, 609 (1991).
- <sup>21</sup>R. D. Johnson, C. S. Yannoni, H. C. Dorn, J. R. Salem, and D. S. Bethune, *Science* **255**, 1235 (1992).
- <sup>22</sup>G. Harbottle, in *Effects of Nucleogenesis Preceding Chemical Reaction: Dissipation of Excitation Before Chemical Reaction*, edited by G. Harbottle and A. G. Maddock, *Chemical Effects of Nuclear Transformations in Inorganic Systems* (North-Holland, Amsterdam, 1979).